Translational Research in Anatomy xxx (2015) 1–9

Contents lists available at ScienceDirect

Translational Research in Anatomy

journal homepage: http://www.journals.elsevier.com/translational-research-in-anatomy

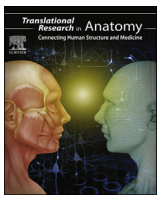

Mouse models of spinal cord injury and stem cell transplantation

Aman Deep [a], Nimer Adeeb [a, d], Nicole Hose [a], Mona Rezaei [a], Salman Abbasi Fard [a], R. Shane Tubbs [b], Parham Yashar [a], Mark A. Liker [d], Babak Kateb [a, c], Martin M. Mortazavi [a, *]

[a] California Neurosurgical Institute, Thousand Oaks, CA, USA
[b] Seattle Science Foundation, Seattle, WA, USA
[c] Society of Brain Mapping and Therapeutics, Santa Monica, CA, USA
[d] Department of Neurological Surgery, Keck School of Medicine, University of Southern California, Los Angeles, CA, USA

ARTICLE INFO

Article history:
Received 22 February 2015
Received in revised form
12 October 2015
Accepted 12 October 2015
Available online xxx

Keywords:
Spinal cord injury
Models
Mouse
Stem cells
Therapy
Transplantation

ABSTRACT

Spinal cord injury is one of the most devastating neurologic conditions that mostly affects young, and otherwise healthy, patients. Following the primary phase of injury, deleterious secondary inflammation and vascular disruption lead to a more sustained and permanent damage. Over the years, various animal models of spinal cord injury have been developed to help understand the mechanism and the pathophysiology of injury, and to develop reliable treatment strategies. These animal models, especially for the mouse, have also become the target of stem cell therapy, which aims to replace the lost cellular element at the site of injury. In this review, we will discuss the different types of mouse models of spinal cord injury, and elaborate on the therapeutic use of stem cells transplantation.

Contents

* Corresponding author. California Neurosurgical Institute, 77 Rolling Oaks Drive, Suite 203, Thousand Oaks, CA 91361, USA.
E-mail address: M_Mortazavi@hotmail.com (M.M. Mortazavi).

http://dx.doi.org/10.1016/j.tria.2015.10.001

Please cite this article in press as: A. Deep, et al., Mouse models of spinal cord injury and stem cell transplantation, Translational Research in Anatomy (2015), http://dx.doi.org/10.1016/j.tria.2015.10.001

1. Introduction

Spinal cord injury (SCI) is a devastating condition that may result in a permanent neurological damage ranging from minor deficit, to hemiplegia, quadriplegia, and death. Despite the extensive and rapid advancement in medicine, there is still no effective therapy. Over the last two decades, stem cell therapy has attracted great attention for treating SCI by replacing the lost cellular and supporting elements [20,21]. Different types of stem cells at various stages of maturation have been used. Nevertheless, the safety and efficacy of this method has not been well established in humans to date and further animal studies are needed. The mouse model of SCI has been greatly utilized for spinal cord research purpose. This animal-based research can give insight into human research, despite the differences between the two types of cells.

Herein, we will discuss the different types of mouse models of SCI, with emphasis to the prominent studies performed on these models.

2. Chronological development of animal models of spinal cord injury

The first experimental generation of SCI in animal models was performed by Schmaus [26], who studied the effect of concussion on rabbit spinal cord. The injury was induced by tying a wooden board on a rabbit's back and performing a blow trauma to the board. Thereafter, various mechanisms for inducing SCI in different animal models were innovated [34].

Allen [2] developed a weight drop method to induce a spinal cord contusion model in canines. The injury was induced by dropping a weight from a measured height through a perpendicular tube on the exposed spinal cord with intact dura mater. Ayer [4] produced compression injury of spinal cord by injecting paraffin into the epidural space of feline spinal cord. McVeigh [19] produced compression injury in dogs via the fingertip. Thompson [32] produced crush injury in cats' spinal cord via a fingertip and scalpel handle. Ferraro [10] induced spinal cord concussion in rabbits by applying a blow to the back with an iron rod. Craig [7] produced compression injury in cat spinal cords by inserting pieces of bone wax into the intradural space around the spinal cord.

Tarlov et al. [31] developed a hydraulic compression device to produce both acute and chronic compression injuries in dogs. Rubber hydraulic balloons were inserted into the epidural space to produce quantitative degenerative lesions. Gelfan and Tarlov [12] postulated that the conduction block caused by canine spinal cord compression was reversible and was directly related to mechanical deformation rather than anoxia. Coe et al. [6] induced cervical spinal cord flexion compression in a rhesus monkey, by rigid fixation of the head with body acceleration. Harvey and Srebnik [13] induced spinal cord crush injury in rats, using thumb forceps. Ducker and Hamit [9] developed a beagle model of spinal cord contusion, using the weight drop technique. Kelly et al. [15] induced spinal cord contusion in dogs, and reported significant recovery following treatment with hypothermia and hyperbaric oxygen. Yeo and Payne [36] and Yeo et al. [35] developed a contusion model of SCI in sheep by weight drop. Sheep spinal cord more closely resembles the spinal cord of humans compared to other animal models, especially in terms of size. DeGirolami and Zivin [8] developed a spinal cord ischemia model in rabbits by placing a polyethylene catheter around the aorta distal to the renal artery. Sholomenko and Steeves [29] induced a variety of hemisection SCI in Canadian geese and Peking ducks. Wrathall et al. [33], have introduced modifications to the original weight drop method of Allen [2] and used a device in which a weight is dropped along a vertical rod on an impounder applied to the spinal cord. Their technique has been one of the most popular techniques of inducing SCI due to being simple and cheap. Blight [5] developed a guinea pig model of spinal cord compression, by using a modified pair of forceps.

3. Mouse models of spinal cord injury

Mouse models of SCI offer the advantage of being cost effective in terms of buying and maintaining the samples [17]. Moreover, mice are exposed to a diversity of natural mutations as well as genetically engineered ones, which offer a wider scope of possibilities for research.

3.1. Graded contusive model using weight drop method

Kuhn and Wrathall [17] developed a mouse model of graded contusive SCI using a weight drop method. Contusive models of SCI are most appropriate in terms of mimicking human injuries, which are mostly caused by non-penetrating blunt trauma (e.g., fall, vertebral dislocation, and burst fracture). Their method was modified from the impounder weight drop technique used by

Please cite this article in press as: A. Deep, et al., Mouse models of spinal cord injury and stem cell transplantation, Translational Research in Anatomy (2015), http://dx.doi.org/10.1016/j.tria.2015.10.001

Wrathall et al. [33] in rats. Following laminectomy, transverse processes around the area where the impounder will be applied are clamped with McPherson forceps to achieve spinal column stabilization. A nylon impounder with a tip diameter of 1.5 mm is applied against the spinal cord. The nylon impounder is loosely fitted over the end of a brass rod that is inserted through the weight. The brass rod itself is attached to a stereotactic frame for precise positioning. Fine adjustment of surgical planes can be performed with a microscope mounted overhead and attached to the rod that supports the impounder. The weight used in this study for contusive injury ranged from 1 gm × 2.5 cm to 3 gm × 5 cm.

3.2. Graded contusive model using pneumatic impact device

Seki et al. [28] developed a contusive SCI model using a pneumatic impact device, which was modified from the weight drop device. The advantage of pneumatic compression device over the weight drop method is the precise control of impact and biomechanical monitoring of variations associated with impact injury. Rate, depth, and duration of impact are controlled precisely, and the bouncing effect on dura, which is a major drawback in the weight drop method, is eliminated with the pneumatic impact model.

The pneumatic impact device consists of a 1.5 mm bore, double acting, pneumatic cylinder with a 5 cm stroke. The cylinder is mounted vertically on a cross bar that can be adjusted along the vertical axis. The impactor is mounted on the lower end of the rod and is applied against the spinal cord. The transducer core of a linear variable differential transformer is attached to the upper end of the rod. A time displacement curve is used to measure the impact velocity. Between 1 and 4.4 m/s range of impact velocity can be generated by applying a controlled gas pressure to the impactor. Controlled gas pressures of 12, 20, and 45 psi when applied to the impactor can generate velocities of 1, 2, and 3 m/s, respectively. The SCI produced is directly related to the impact velocity, total time of impact, and depth.

3.3. Spinal cord ischemic injury model

Spinal cord ischemia is a devastating complication of aortic aneurysm repair, aortic rupture, and dissection of the aorta, and may lead to acute or delayed paralysis. To study the histopathologic changes, various animal models of spinal cord ischemia have been developed. The most popular is the rabbit model developed by DeGirolami and Zivin [8]. In this model, the infrarenal segment of the aorta was occluded, leading to paraplegia. The major drawback of this model is its difference from spinal cord ischemia mechanism in humans. In humans, infrarenal occlusion of the aorta does not cause paraplegia because spinal cord at the thoracolumbar level is supplied by the artery of Adamkiewicz, which arises from left posterior intercostal arteries, mostly between T8 and L1.

Lang-Lazdunski et al. [18] developed the first mouse model of spinal cord ischemia. Spinal cord ischemia in mice mimics that of humans due to the similarity in vasculature, with one anterior and two posterior spinal arteries, and heterosegmental radicular arteries.

In their model, the left internal mammary artery and aortic arch between the left subclavian and common carotid arteries were occluded with a clip. Within 15 s of occlusion, another clip was applied at the origin of the left subclavian artery. Occlusion was applied for 9 min (Group A) and 11 min (Group B), after which clips were removed. Motor function was assessed at 0, 1, 3, 6, and 24 h after removal of occlusion clips. Both study groups became acutely paraplegic. In Group A, motor function recovered within 24 h of occlusion, while in group B, 80% showed complete paralysis.

Histologically, spinal cord sections at T5 to T7 showed no changes, while L1 to L5 showed changes in all the sections. In group A, the dorsal horn was maximally affected. The intermediate gray matter was also affected. The ventral horns were minimally affected. Less than 10% of motor neurons had eosinophillic cytoplasm. In group B, dorsal horns and intermediate gray matter had comparatively more red neurons, and more than 50% of motor neurons were eosinophillic. Only group B had parenchymal edema.

With the ventral surgical approach described by Lang-Lazdunski et al. [18], it was difficult to isolate aortic arch and left subclavian artery from the adjacent tissue, to achieve complete occlusion for the application of the clip. Furthermore, with this approach, it was difficult to separate the vagus nerve from the left subclavian artery without damaging it, which has resulted in a high mortality rate. To overcome this drawback, Awad et al. [3] used a lateral thoracotomy approach, which facilitated the separation of vessels and nerves, and allowed for easier access to the descending aorta for complete occlusion.

In comparing their method to the ventral surgical approach of Lang-Lazdunski et al. [18], the lateral approach by Awad et al. [3] was associated with a mean survival of 68 h after clip application for 3–11 min, compared to 39 h following the ventral approach. With lower body temperature, there was a significant increase in mean survival, reaching up to 63 days at 33 °C and clip application for 7.5 min.

3.4. Photochemical graded ischemic injury model

Gaviria et al. [11] developed a mouse model of photochemical graded spinal cord ischemic injury. After the exposure of laminae and spinous processes of T8-T10, the spinal cord was exposed to Xenon lamp irradiation beam (560 nm wavelength), focused through fiber optics. Animals were sacrificed at day 1 or 7 post injury, and were divided into five groups according to the size of the fiber optics and the duration of exposure. 1- Animals irradiated for 5 min with 5 mm fiber optic exposure showed loss of 30% of mean gross motor function, and impairment of 30% of bladder and mean reflective functions. The nociceptive response was mild to moderately increased. 2- Animals irradiated for 6 min with 5 mm fiber optic exposure showed 50–75% loss of mean gross and fine motor function, 80–90% impairment of bladder function, and 70–80% impairment of mean reflective function. Nociceptive response increased to 40%. 3- Animals irradiated for 6 min with 3 mm irradiation showed similar outcome as 5 min with 5 mm fiber optic irradiation group animals. There was mild to moderate impairment of functions. 4- Animals irradiated for 7 min with 3 mm irradiation showed loss of 50–60% of mean gross motor function, 80% decrease in mean fine motor function, and impairment of 80% of bladder function, 40–70% of mean reflective functions, and 80% of mean proprioceptive function. The nociceptive response was increased to 20–30%. 5- Animals irradiated for 8 min with 3 mm irradiation showed loss of 70–90% of mean gross motor function, 90% decrease in mean fine motor function, and impairment of 100% of mean bladder function, 80–100% of mean reflective function, and 100% of mean proprioceptive function. The nociceptive response was increased to 10–50%. In animals that were moderately-to-severely injured, that is, irradiated for 5–8 min, the most commonly affected anatomic region was the entire dorsal funiculus. In severely injured animals, almost the entire spinal section was affected, including dorsal horns, central canal, lateral funiculus, ventral horns, and ventral white maters.

Histologically, there was absence of cavitation and necrosis at the photochemical lesion site. Neural tissue was replaced by cellular and extracellular matrix confirmed by Luxol fast blue and Nissl-stained glial fibrillary acidic protein (GFAP) labeling. During the early phase post injury, the site was edematous with neutrophil

Please cite this article in press as: A. Deep, et al., Mouse models of spinal cord injury and stem cell transplantation, Translational Research in Anatomy (2015), http://dx.doi.org/10.1016/j.tria.2015.10.001

and platelet infiltration in the fibrin clot. During the late phase, the lesion site was infiltrated by macrophages, fibroblasts, endothelial cells, and polymorphoneuclear cells.

3.5. Transection model

Seitz et al. [27] developed a spinal cord transection mouse model. The aim of this model was to minimize the scar formation after the injury, which is a major block for the regeneration capability of the nervous system. In their study, two types of surgeries were performed. In the first group, the dura was left open, and in the second group, the dura was left intact. In the "cut dura" group, the spinous processes of T8-10 were exposed by a 1.3 cm dorsal median incision. A forceps was used to hold the spinous process of T8 or T9 and was lifted to open the intervertebral space. Complete transection of the spinal cord was achieved using a micro scalpel. The incision was performed by moving the scalpel from right to left and again from the left to right directions with the tip of the scalpel moving over the osseous part of the spinal canal to ensure complete transection.

In the 'intact dura' animals, the micro scalpel blade was modified to a size of 0.4 mm high and 5 mm long. After a 0.5 mm longitudinal incision of the dura, complete transection of the spinal cord was achieved by inserting the blade between the spinal cord and dura towards the right side and cutting the complete circumference of spinal cord. Complete transection was confirmed by sliding the blade against the osseous surface of the spinal canal.

The Basso, Beattie, and Bresnahan (BBB) scale was used to assess the motor function at 1, 4, 7, 14, and 21 days post surgery. Both groups showed recovery within the first 3 weeks. In the 'intact dura' group, animals started moving their hindlimbs in two weeks, and more than half of the animals showed improvement, and scored 15–20 points on BBB scales within 3 weeks. To rule out reflex automatism as the cause of improvement, two animals that showed recovery were re-injured and showed no hindlimb movement immediately and 2 weeks post re-injury. In the 'cut dura' group, there was extensive fibroblast infiltration and increase in the gap between the cut ends of spinal cord. On the contrary, in the 'intact dura' group, scarring was prevented. The infiltration and collagen were less dense. Retrograde tracing was performed after 2 weeks of injury in 2 animals of the 'cut dura' group that scored 0 on the BBB scale, and 2 animals from the 'intact dura' group that scored 15 on the BBB scale.

Two weeks after injury, 0.1 μl of 5-(and-6)-Tetramethylrhodamine in 5% solution of phosphate-buffered saline (PBS) was injected under pressure using a 20 μm pulled glass micropipette on both sides of gray matter of the lumbar enlargements. Each injection lasted for 5 min and the pipette was left for another five minutes before it was withdrawn. Five days after the injection, animals were perfused, and 15–20 μm frontal sections of cortex and brainstem, and longitudinal section from the site of injection were performed. Specimens with tracer leakage in subarachnoid space and area above the injection site were excluded. In the 'intact dura' model, retrograde-labeled neurons were seen in considerable numbers. The nucleus vestibularis lateralis, nucleus ruber, nucleus raphe, and nucleus gigantocellularis alpha were labeled with tracer. In the 'cut dura' group, one animal showed no labeled neurons and the second animal showed minute labeling in nucleus gigantocellularis and nucleus vestibularis lateralis. Few labeled neurons in the hindlimb-corresponding cortex of the 'intact dura' group were seen, in contrast to not-labeled neurons in the 'cut dura' group.

3.6. Graded forceps crush model

Plemel et al. [24] developed a spinal cord crush model using forceps. The aim of this model was to produce varying degrees of SCI using forceps with spacers, which help in controlling the force of impact on the spinal cord. The width of the forceps blades was adjusted to 0.5 mm. Spacers were placed between the blades, so once the forceps closes, it creates a varying closure distance that compresses the cord to the thickness of 0.25 mm, 0.4 mm, and 0.55 mm, graded as mild, moderate, and severe, respectively. T6–T7 laminectomy was performed, and dura was kept intact. The compression was maintained for the duration of 15 s. A sham group was also included. After recovery, field locomotion, foot print and horizontal ladder paradigms were used to assess the hindlimb motor functions. Post surgical day 2, 4, and 7 were used for open field assessment, which was performed on a weekly basis thereafter. Open field locomotor assessment was performed using Basso mouse scale (BMS), which was deemed to be more sensitive than the BBB for mouse locomotion testing, with inter-rater reliability of 0.5.

On assessment, the mild injury group (0.55 mm) scored an average of 8.6 ± 0.12 on BMS. This group showed only abnormal tail position or instability of the trunk. The moderate injury group (0.4 mm) scored an average of 7.6 ± 0.51 on BMS. The animals achieved coordination between the forelimbs and hindlimbs, plantar stepping, and parallel paw placements, but the animals were unstable and rotated their paw while lifting it up. The group with severe injury (0.25 mm injury) scored an average of 4.2 ± 0.57, which signifies that the animal performed occasional plantar stepping.

Tissue analysis was performed by using immunoreactivity to GFAP-specific antibody. In the mild injury group, $GFAP^-$ tissue was present in gray matter and lateral columns of the lesion. In the moderate injury group, $GFAP^-$ tissue was present throughout the gray matter sparing only a rim of white matter in the spinal cord. In the severe injury group, $GFAP^-$ tissue was present throughout the site of injury sparing only peripheral patches of $GFAP^+$ tissue, which showed enhanced astrocytic reaction.

Myelin basic protein (MBP)-immunoreactivity was used to analyze the myelin disruption. The mild injury group showed myelin degeneration in the lateral funiculus at the epicenter of the crush injury. Myelin was normal at 800 μm rostral and caudal to the epicenter. The moderate injury group had central degeneration with a spared white matter rim, the tissue caudal and rostral to the lesion epicenter showed patchy degeneration. In the severe injury group, myelin was absent at the epicenter of crush injury. The white and gray matter was significantly degenerated 1200 μm rostral and caudal to the lesion.

To compare the cytoarchitecture of lesions among the groups, laminin and fibrin immune-staining was performed. Mild injury group had less than 0.2 mm^2. The lesion site was filled with phagocytes, surrounded by laminin and fibronectin immunoreactive material. The moderate injury group had $laminin^+$ cells that bridged the spared rim of spinal cord tissue. The severe injury group had laminin and fibronectin staining occupying the entire injured site.

4. Neural stem cells

4.1. Neural stem cells derived from embryonic stem cells

4.1.1. Introduction

Okada et al. [22] described the modified in vitro technique to induce neural stem cells (NSC) using mouse embryonic stem cells (ESC). Until that time, mid to late gestational or adult brains were used to obtain the NSC, but the plasticity in these cells was limited. The older protocols had to be changed according to the cell type, and they also lacked the ability to evaluate the association between

Please cite this article in press as: A. Deep, et al., Mouse models of spinal cord injury and stem cell transplantation, Translational Research in Anatomy (2015), http://dx.doi.org/10.1016/j.tria.2015.10.001

spatial and temporal identities using the same culture system. These protocols were also vulnerable to contamination by non neural cells and various undifferentiated cells. In the new protocol there was no need to add leukemia inhibitory factor (LIF) to keep the embryonic stem cells in an undifferentiated state, and the floating culture technique allowed the formation of embryoid bodies (EB).

4.1.2. Methods

In this study [22], standard ESC medium with 0.1% gelatin coated tissue culture dishes were used to produce neurospheres from ESC through EB formation. Noggin in a concentration range of 0–10 μg and/or retinoic acid 0–2 × 10^{-6} M were added. Retinoic acid acts as a neural inducer of ESC, and also as a caudalizing factor for hindbrain and rostral spinal cord formation. Noggin has a special property of inhibiting bone morphogenetic signaling and inducing forebrain development.

4.1.3. Results

4.1.3.1. Generation of neural stem cells. In their previous experiment [23], the authors found that noggin and retinoic acids in concentration of 10^{-8} M induced Sox1$^+$ and Nestin$^+$ neural progenitors. They also found that post mitotic βIII-Tubulin$^+$ neurons were induced by 10^{-6} M concentration of retinoic acid. In the current experiment, they could produce 2.6 fold (1 μg/ml noggin) and 4 fold (10^{-6} M retinoic acid) more neurospheres. To confirm the origin of neurospheres from NSC and self renewal properties, noggin or low retinoic acid neurospheres (low density culture 2.5 × 10^4 cells/ml) generated the secondary neurospheres when deposited on 96 well plates, which proved their self renewal potential. Basic fibroblast growth factor (bFGF)-containing serum free media with noggin and low retinoic acid was used to culture dissociated EB for 7 days to form primary neurospheres. Primary dissociated neurospheres were then cultured in bFGF and epidermal growth factor (EGF)-containing media for 8–9 days to form secondary and tertiary neurospheres. EB cultured for 4 days at high concentration of retinoic acid (10^{-6} M) produced primary neurospheres but no secondary neurospheres. Immunocytochemical analysis for the markers of neurons (βIII-Tubulin), astrocytes (GFAP), and oligodendrocytes (O4) showed that the majority of the primary neurospheres composed of neurons only and a small number of glial cells. The secondary and tertiary neurospheres contained more glial cells and multipotent colonies, which were consistent with in vivo development, where glial cell generation follows neuronal generation.

Analysis was performed to evaluate clonal neurospheres formation. Monomeric red fluorescent protein (mRFP) or venous expressing lentivirus were used to transduce dissociated EB. They were plated in 1:1 ratio of 0.45–1 × 10^4 cell density and cultured in a hormone mix media (MHM0) containing 0.8% methylcellulose, and bFGF in a concentration of 20 ng/ml, for secondary neurospheres formation.

4.1.3.2. Electrophysiological analysis. Electrophysiological analysis via whole cell patch clamp was performed to test the functionality of neurons. Noggin treated EB-derived neurospheres were allowed to dissociate and differentiate for 10–14 days on Ploy-L-ornithine/fibronectin coated cover glasses before testing. Tests showed transient inward (Na^+) and sustained outward currents (Delayed rectifier K^+). The holding voltage was −60 mV and command voltage ranged from −80 to 50 mV. Transient Na^+ current showed sensitivity to tetrodotoxin. Sustained positive current stimulus resulted in repetitive action potential firing in all the neurons that were being tested. These tests showed that these neurons were electrophysiologically intact.

4.1.3.3. Markers analysis. Rostrocaudal characteristics of neural stem cells were identified by using various concentrations of noggin and retinoic acid. Forebrain and midbrain markers (*Foxg1, Otx1, Otx2, and Enl*) and markers for hindbrain (*Pax2, Gbx2, Hoxb1, Hoxa2, and Hoxb4*) were expressed by noggin and low-retinoic acid neurospheres, respectively. High-retinoic acid neurospheres expressed Pax2$^+$ and Hoxb4$^+$ markers for hindbrain and spinal cord, but not Otx1$^+$ markers for forebrain and midbrain. This further proves that retinoic acid, in a concentration-dependent manner, can drive the caudalization on NSC when added during formation of EB. Noggin and low retinoic acid neurons were positive for choline acetyltransferase (ChAT), glutamic acid decarboxylase (GAD67), GABA, tyrosine hydroxylase (TH) and serotonin (5-HT). High-retinoic acid neurons expressed GAD67$^+$ and ChAT$^+$ but not 5-HT or TH. Dorsoventral identity of NSC was regulated by the addition of sonic hedgehog (SHH), which determined the dorsoventral axis from ventral notochord and floor plate. Wingless (wnt3a) and basic membrane protein (BMP)-4 determined the axis from dorsal roof plate. These secreted factors were added during the formation of neurospheres. Basal forebrain marker Nkx2.1 was expressed by noggin neurospheres treated with 300 nm of SHH, and generated 69.2 ± 8.2% Nkx2.1$^+$ ventral colonies. 50 ng/ml concentrations of Wnt3a-treated neurospheres produced 84.0 ± 3.1% Pax6$^+$ dorsal colonies. Midbrain marker (Gsh2 and Dlx2) expression was unaffected with or without adding SHH or Wnt3a secretory factors. Low-retinoic acid neurospheres (control) normally expressed ventral identity and gave rise to 82.4 ± 5.9% of Nkx6.1 ventral colonies and fewer, 25.7 ± 2.9% of Pax3$^+$, dorsal-identity colonies. The addition of 300 nm SHH further increased the Nkx6.1 ventral colonies to 96.7 ± 1.5%, and addition of Wnt3a in a concentration of 50 ng/ml further increased the Pax3$^+$ dorsal colonies proportion to 51.4 ± 5.8%. High-retinoic acid neurospheres (control) produced very small number of Nkx6.1 ventral colonies and about 44.4 ± 11.7% of Pax3$^+$ dorsal colonies. Addition of 300 nm of SHH increased the Nkx6.1 ventral colonies to 61.2 ± 10.9%, and addition of 50 ng/ml of Wnt3a increased the expression of Pax3$^+$ colonies to 65.5 ± 9.3%. To test the ability of forming synaptic connections, low-retinoic acid neurospheres were generated from ES, which were tagged genetically with green fluorescent protein (GFP). Neuromuscular contacts were expressed by GFP-labeled neurons after labeling with rhodamine α-bungarotoxin.

4.2. Embryonic stem cell-derived neural stem cell transplantation

4.2.1. Preparation of neural stem cells

Kimura et al. [16] described a technique to transplant NSC derived from ESC into the injured spinal cord of an adult mouse. They also investigated the advantage of adding thyroxine (T4) to the therapy. An adult female 129/Svj mouse model was used for the experiment. EB3 ESC-derived G4-2 murine cell line was used for transplantation. G4-2 cells express enhanced green fluorescent protein (EGFP) gene, which is under the control of CAG unit expression. Gelatin coated dishes without feeder cells in DMEM medium were used to maintain undifferentiated G4-2 ESC. The culture media was also enriched with 10% fetal bovine serum (FBS), 10 mM Sodium pyruvate, and 0.1 mM of 2-mercaptoethanol, 10 nM non-essential amino acids and 1400 U/ml of LIH. To eliminate undifferentiated cells, media containing 10 μg/ml of blasticidin was used to culture G4-2 cells. EB were formed from undifferentiated ESC (stage 1) and cultured in hanging drops at a cell density of 500 cells per drop for 4 days without LIF (stage 2). EB adherence was promoted by plating it on gelatin coated tissue culture surfaces for 24 h. ESC medium was replaced by serum free insulin/transferring/selenium/fibronectin media for 7 days to initiate Nestin$^+$ cell selection (stage 3). N2 medium enriched with laminin (1 μg/ml)

Please cite this article in press as: A. Deep, et al., Mouse models of spinal cord injury and stem cell transplantation, Translational Research in Anatomy (2015), http://dx.doi.org/10.1016/j.tria.2015.10.001

and bFGF (10 ng/ml) was used for cell expansion initiation for 6 days (stage 4).

Graft cell characteristics were analyzed using immunocytochemistry. Nestin, oligo 1, GFAP, and MAP2 expression was absent in undifferentiated ESC. Nestin mRNA was expressed by cells in stage 2, MAP2 in stage 3, and the oligo 1 mRNA in stage 4 of culture. After stage 4, the cells were harvested and recultured in media without bFGF, which resulted in early appearance of $MAP2^+$ (neurons) cells within few days along with $O4^+$ (oligodendrocytes) and $GFAP^+$ (glial cells) cells. To prepare the cells for transplantation, the $Nestin^+$ cells, after stage 4, were trypsinized with 0.25% trypsin for 5 min at 37 °C, and dissociated cells were suspended in PBS.

4.2.2. Spinal cord injury model

SCI was created in 10–12-week-old adult female 129/Svj mice. A T9-T10 laminectomy was performed. With the dura kept intact, contusion injury was induced using a pneumatic direct impact device consisting of a 1.0 mm bore pneumatic impactor and 5.0 cm stroke capable pneumatic cylinder. 40 psi of impact pressure was used to achieve an impact velocity of approximately 3000 m/s to create a constant impact depth of 0.5 mm for a duration of 50 msec.

4.2.3. Transplantation

Mice were divided into three groups. Group I mice received no treatment. Group II and III were transplanted with 2×10^4 graft cells in 2 μl of PBS into the injured site, 10 days post SCI. Group III mice were also transplanted with an intraperitoneal osmotic mini pump which contained 0.2 ml of T4 solution for continuous 14 days injection. To prepare T4 solution, 5 mg of I-T4 was mixed in 0.1 N NaOH (1 ml) and 0.15 ml of T4, NaOH solution was mixed in 100 ml of normal saline to achieve final concentration of 7.5 μg/ml. The pump was re-implanted intraperitonially after 14 days to achieve continuous 28 days infusion of T4. On the 28th day after the transplantation, immunohistological analysis of the spinal cord was performed.

4.2.4. Behavioral assessment

Behavioral assessment was performed at day 1 and one week after the injury and again 7, 14, 21, and 28 days after the transplantation. Mice were trained and selected randomly for the assessment. Three scoring parameters were used: (1) Motor score, by testing coordinated motor function in an open field with score range from 0 to 6; (2) Platform hang, which assesses the ability of mice to climb on the top of a platform with the help of hindlimbs with forelimbs placed on the edge of the platform with score ranges from 0 to 4; and (3) Rope walk, to assess the ability to navigate a 15 inch long, ½ inch wide sisal rope suspended 1 foot above the bedding, with the score range from 0 to 4 points. Significant improvement was shown by Group II and III on days 21 and 28. There was no significant difference between group II and III throughout the 4 week assessment. Injection of thyroxine did not show any advantage.

4.2.5. Histological analysis

On day 28, mice were euthanized and the spinal cord was fixed in 4% paraformaldehyde in PBS at 4 °C for 24 h and then transferred to 10% and 15% sucrose in PBS at 4 °C for 4 h each, followed by 20% sucrose in PBS at 4 °C overnight. Specimens were cut in 10 μm slices with cryostat and mounted on 3-aminopropyltriethoxysaline coated slides. These slides were rinsed in PBS and incubated in anti-GFP in 1:9000 dilution, anti-Tuj1 in 1:2000 dilution, anti-Nestin (1:500), and anti-O4 (1:1000) with 0.1% triton (X-100) overnight at 4 °C. After overnight incubations, sections were rinsed in PBS incubate for 60 min in media containing Rhodamine (1:200), a fluorescent-labeled secondary antibody with 0.1% Triton X-100. These sections were again rinsed in PBS and mounted and cover slipped for evaluation with laser confocal microscope. In Group I, empty cavity was seen with reactive astrocytosis and loss of volume on dorsal aspect of spinal cord. In Group II, there was no cavity at the transplanted site and astrogliosis was less prominent on the edges. $GFAP^+$ cells were present in the cavity. Among the $GFAP^+$ cells, $Tuj1^+$ and $O4^+$ cells were present suggesting that embryonic cell-derived neural stem cells differentiated into neurons and oligodendrocytes. Few axons from the graft sprouted and few axons were also seen penetrating the graft, but there was clear demarcation between the spinal cord and graft. There was no tumor formation in any of the groups. There was no difference between group II and III.

4.3. Induced pluripotent stem cells

Due to the ethical issues associated with the use of human ESC, there was a great need to find alternate source of stem cells. Takahashi et al. [30] made a breakthrough by generating induced pluripotent stem cells (iPSC) from mouse and human fibroblasts, using retrovirus containing human pluripotency-related transcription factors (i.e. Oct3/4, Sox2, Klf4, and c-Myc).

The generated iPSC expressed surface antigens specific to ESC, including TRA-1-60, TRA-1-81, TRA-2-49/6E, NANOG Protein, SSEA-3, and SSEA-4. Currently, further studies are being conducted on iPSC as a promising substitute to ESC, and to test their safety and efficacy.

4.4. Epidermal neural crest cells

4.4.1. Introduction

Epidermal neural crest stem cells (EPI-NCSC) represent the remnant of embryonic neural crest stem cells. Postnatally, they are found in bulge of hair follicles. EPI-NCSC have been shown to express neuronal, GABAergic, and oligodendrocytes markers but lack astrocytes or Schwann cells markers. These cells do not form tumors or teratoma at the transplant site.

4.4.2. Isolation and culture

In the study of Hu et al. [14]; EPI-NCSC were used to repair SCI in mouse. Wild type C57BL6/J and C57BL/6-TgN (ACTbEGFP)1Osb mice, which expresses EGFP, were used for the experiment. 10–12 weeks mice were used to acquire bulge explant from whisker follicles. After dissecting the whiskers, tungsten needles were used to scrape the connective tissue from the follicle and rinsed to expose the ring sinus and cavernous sinus. Longitudinal cut was made in the capsule and then cut above and below the bulge to remove the bulge out of capsule. Collagen-coated plates with culture media containing 85% α-modified MEM, 10% fetal calf serum, and 5% day11 chick embryo extract were used to grow bulge explants. Within 3–4 days, cells started to migrate from the bulge. Bulge was removed from the media and the cells were trypsinized and subcultured.

4.4.3. Transplantation

T8 laminectomy was performed. Moderate SCI in the midline was induced with a modified Newton meter at a force of 12 centi-Newtons for a duration of 3 s 0.8 μl of EPI-NCSC was injected on the left side of spinal cord to both rostral and caudal margins, to bridge the lesion. Injections were made for a duration of 4–5 min. Approximately $1.4 \times 10^5 \pm 2.3 \times 10^4$ cells per mouse were injected.

4.4.4. Electrophysiological study

Spinal Evoked Potential (SpSEP) were recorded for 19 mice with SCI and EPI-NCSC graft, 22 mice with SCI and saline injection, and 6

Please cite this article in press as: A. Deep, et al., Mouse models of spinal cord injury and stem cell transplantation, Translational Research in Anatomy (2015), http://dx.doi.org/10.1016/j.tria.2015.10.001

mice with no injuries for a duration of 4 months following injury. To do the recording, animals were anaesthetize and two Teflon wires with 7-strands (0.0254 mm diameter with 3 mm deinsulation region) were placed subcutaneously, rostral to the injury at T4-level. High input impedance module (2 TΩ) and 10 pF capacitance were used to record from the electrodes. 23G needle was placed subcutaneously for stimulation, 3 cm caudal to the caudally placed recording electrode, and to serve as anode. A 23G blunt needle was placed in popliteal fossa to stimulate the tibial nerve. The tibial nerve was stimulated at 3.5 Hz frequency for pulse duration of 500 μs and intensities of 1×, 2×, and 3× with a constant current stimulator. Motor threshold ranged between 0.47 and 0.49 mA in all groups. Each leg and stimulation intensities were used for recordings. The analysis of SpSEP was performed 4 month after injury. Uninjured group showed SpSEP of 29.08 ± 7.3 μV in the right hind leg and 29.9 ± 5.1 μV in the left hind leg. In the group with SCI and saline injection, SpSEP readings were 6.39 ± 2.0 (right hind leg) and 6.05 ± 2.1 (left hind leg) μV. In the group with SCI and EPI-NCSC graft, the SpSEP readings were 12.86 ± 3.5 μV in the right hind leg and 13.27 ± 3.1 in the left hind legs. This group showed 44.4% of SpSEP spinal cord response compared to the uninjured mice.

To check the cutaneous sensitivity, Semmes-Weinstein touch test was used. It consisted of varying thickness filaments with weight ranging from 0.008 to 300 g. Middle of the paw was pressed with filament tip at a 90° angle for a duration of 1.5–2 s. Response was recorded in form of clasping reflex. Gap of 2 min was used in between the tests to avoid desensitization. In non-injured mice, the threshold response in the right hind leg was 7.3 ± 0.8 g and 7.7 ± 0.9 g in the left hind leg. In the group with SCI and saline injection, the response was 141 ± 50.2 g in the right hind leg and 242.2 ± 29.9 in the left hind leg. In SCI group with EPI-NCSC graft, the threshold response was 5.2 ± 0.5 in the right hind leg ($p = 0.0001$) and 5.2 ± 0.5 ($p = 0.0001$) grams in the left hind leg, which shows bilateral recovery of cutaneous sensitivity.

4.4.5. Histological analysis

To prove the differentiation of EPI-NCSC graft into myelinating oligodendrocytes, immuno-electron microscopy was performed. After anesthesia, the animals' spinal cord lesion site was exposed, and 4% paraformaldehyde drops were placed at the level of injury and on spinal cord. Ten minutes after this procedure, mice were euthanized, and the spinal cord with injury site was removed and incubated for 30 min in 4% PFA in 0.1 M phosphate buffer at a pH of 7.3. Fluorescence microscopy was performed to visualize EGFP signal. The fluorescent sections were cut into 200 μm sections and froze in high pressure freezing apparatus and were placed in ethanol, in 0.5% uranyl acetate, and then into Lowicryl K11M resins. Ultrathin sections of the specimen were mounted on formvar-coated grid. These sections were probed with anti-GFP polyclonal rabbit serum. Goat anti-rabbit 10 nm gold probe was used to visualize anti-GFP antibody. Retrograde tracing was performed to check the connections between the grafted cells and spinal cord. Alexa Fluor 680-conjugated dextran was used for tracing and its retrograde transport suggested that neurites from the injured spinal cord were able to traverse the scar. Also the EPI-NCSC derived cell bodies and neuritis show a red fluorescence. Green florescence grafted cells with no red fluorescence were also present.

4.5. Valproic acid and neural stem cell transplantation

4.5.1. Introduction

Valproic acid (VPA) is an anti-epileptic and mood stabilizing drug used primarily for epilepsy and bipolar disorders. Recently, VPA has been found to be a direct inhibitor of histone deacetylase and resulted in hyperacetylation of histones in teratocarcinoma. VPA also suppress differentiation of astrocytes and oligodendrocytes, but, on the other hand, it acts as a neuronal differentiation inducer.

4.5.2. Method

4.5.2.1. Isolation and culture. Abematsu et al. [1] have combined Valproic acid with transplanted NSC to aid recovery in SCI. Three different Tg mouse lines were used to produce NSC from embryonic forebrains. GFP (GFP-Tg), GFP & LUC (GFP.LUC-Tg), and/or GFP, LUC and diphtheria toxin receptor (TR6.GFP.LUC-Tg) were among the factors expressed by these mouse cell lines. Expression of these factors helps in the differentiation of host cells from NSC. Toxin receptor-mediated conditional knock out procedure (TRECK) was used for the ablation and visualization of the target cells. NSC stem cells derived from E14.5 forebrains were used for transplantation. E14.5 forebrains were derived from mice which were heterozygous for GFP and LUC, TR6.GFP and LUC, and GFP. To obtain NSC, E14.5 forebrains were dissected and Hank's balanced salt solution (HBSS) was used to triturate the forebrains, which were then plated on N2 DMEM/F-12 and 10 ng/ml bFGF containing poly-ornithine and fibronectin coated dishes for a duration of 4 days. The cells were again placed on polyornithine and fibronection coated dishes in NS-A medium supplemented with 10 ng ml of bFGF and EGF. The whole process was repeated 5 to 10 times and the final cells obtained were used for transplantation. These NSC were positive for MAP2ab (neurons), GFAP (astrocytes), and MBP (oligodendrocytes).

4.5.2.2. Transplantation. Fifteen week old male ICR mice (37–45 g) were used for SCI model. T9 and partial T10 laminectomy was performed. After exposing dura, the spinal cord was injured by an impactor device using 90 kilodyne force. NSC were transplanted into the injured spinal cord 7 days after the impact injury. Micropipettes were used to inject 2 μl of NS with no growth factor and supplemented with or without NSC in concentration of 0.5×10^6/μl at 1 μl/min. Cyclosporine in a dose of 8 mg/kg was given to both groups to suppress the immunity. Mice were also injected with VPA in a dose of 150 mg/kg (group I), and saline (control group) for 7 days following transplantation of NSC.

4.5.3. Results

4.5.3.1. Behavioral assessment. BBB scale was used to evaluate hindlimb movements for the duration of 14 weeks post SCI. Hindlimb function in control group mice did not show much improvement (BBB score of approximately 4), but the mice treated with NSC and VPA showed significant improvement (BBB score 9 to10). All the mouse groups transplanted with three different NSC showed comparable data with no significant difference. The recovery from injury reached its peak at 6 weeks post SCI and remained sustained for duration of 3 months.

To check whether the functional recovery was due to host corticospinal tract axon (CST) extensions or due to extension of neuronal processes from transplanted neuronal cells, biotinylated dextran amine (BDA) was injected into the right and left motor cortices (2 μl per cortex). BDA is an anterograde label, and only first grade neurons can be tagged with it. No CST axons were present in the caudal site of SCI in control group and NSC and VPA-treated group, which clearly indicates that CST re-extension was not the cause of improvement. To see if transplanted NSC contributed to the functional recovery, it was found that the transplanted cells in the VPA and NSC treated groups migrated both dorsally and ventrally and also extended their processes to the gray matter and dorsal funiculus 5 weeks after transplantation.

The regeneration of disrupted circuitry connections was confirmed by injection of wheat germ agglutinin (WGA), which is a tracer for neuronal pathway and can be transported trans-

Please cite this article in press as: A. Deep, et al., Mouse models of spinal cord injury and stem cell transplantation, Translational Research in Anatomy (2015), http://dx.doi.org/10.1016/j.tria.2015.10.001

synaptically to second and third generation neurons. Twelve weeks after the SCI, adenovirus with WGA expression was injected into the motor cortex of the mice. In uninjured mice, WGA was traced throughout the ventral horn of spinal cord in the form of intracellular granules in neurons. In SCI group with no treatment, tracer was absent caudally below the level of the injury. In SCI group treated with NSC and VPA, WGA granules were found in the caudal neurons and also in the transplanted neurons in and close to the injury site, which confirmed that the transplanted neurons reconstruct the neuronal circuits. In SCI groups with only NSC transplantation, WGA^+ neurons were higher in number than the untreated group but lower than the group with NSC and VPA treatment.

4.5.3.2. Histological analysis. Immunohistochemical analysis of transplant-derived neurons showed the expression of vesicular glutamate transporter (VGLUT)-2 in 16.9% ± 2.3% neurons and glutamic acid decarboxylase (GAD)-65 in 70.1% ± 1.8% neurons, which are markers for glutamatergic and GABAergic neurons, respectively, and shows that both excitatory and inhibitory neurons were generated from the transplanted NSC. To confirm if the functional recovery was a result of neurons from the transplanted cells, ablation was performed by diphtheria toxin. All the neurons derived from TR6.GFP.LUC-NSC were ablated and the BBB score from group with TR6.GFP.LUC-NSC and VPA decreased to the level of score from untreated and VPA only-treated mice, which support the hypothesis that the functional recovery was contributed to the transplanted neurons and VPA administration. To see if both endogenous and neurons derived from transplanted cells contributed to hindlimb functional recovery, neurons in the gray matter were ablated 12 weeks after SCI by injecting NMDA (0.5 ml in a concentration of 10 mM) at T9 vertebral level. NMDA is an axon sparing excitotoxin. Bilateral injections were made in 5 GFP.LUC-NSC with VPA treatment group, 3 TR6.GFP.LUC-NSC and VPA group, and 3 untreated mice group. The NMDA injection did not cause any change in hindlimb function of uninjured mice, but in treatment groups the functional recovery was completely reversed, which indicate that both endogenous neurons and neurons derived from transplanted cells contributed to hindlimb functional recovery.

4.5.3.3. Role of valproic acid. To confirm the neuroprotective effect of VPA, both cultured and transplanted neurons were treated with VPA and Valpromide (VPM). VPM is a VPA amide analog which do not inhibit histone deacetylase. VPA promoted both neuronal differentiation and growth of neuritis from the transplanted NSC, but inhibited the differentiation into astrocytes and oligodendrocytes. VPM did not result in differentiation of neurons and acetylation of histones, which clearly suggested that histone deacetylase inhibition is an important factor in the differentiation of transplanted neurons. Similarly, the histone acetylation was greatly increased in transplanted cells in injured spinal cord. With VPA treatment, the transplanted cells were also differentiated into neurons rather than glial cells at 1 week and 5 weeks after the SCI. At 5 weeks, there was enhancement of the number of cells positive for MAP2, which is a late differentiation marker for neurons. On the contrary, VPM did not show any differentiation of neurons or improvement of hindlimb motor functions, which further strengthen the hypothesis that inhibition of histone deacetylase is a major contributory factor in neuronal differentiation.

4.6. Neural stem cell transplantation in chronic spinal cord injury

4.6.1. Method

Salazar et al. [25] transplanted human NSC (hNSC) in NOD-*scid* mice 30 days post SCI to detect functional recovery at an early chronic SCI stage. NOD-*scid* mice is an immunodeficient strain that lacks complements, T-cell, and B-cell response, and does not express graft rejection. 16–20 weeks old fetal brain tissue was used to isolate and culture hNSC. *Fluorescence-activated cell sorting* (FACS) technique was used to produce single cell suspension.

4.6.1.1. Isolation and culture. The culture media contained FGF, EGF, LIF, N-acetyl cysteine (NAC), neural survival factor-1, and ex-vivo media with N2 supplement. To grow the human fibroblast (hFbs) from fetal liver, MDM in 10% FBS was used. 50,000 cells/μl concentrations were produced after washing and dissociation by trypsinization. 8–10 weeks old female NOD-*scid* mice were used for SCI model, and were divided into three groups: SCI group transplanted with vehicle, SCI group with hNSC, and SCI group transplanted with hFbs.

4.6.1.2. Transplantation. After T9 laminectomy, contusion injury was inflicted using Infinite Horizon (IH) impactor with a force of 50 kilodyne. Thirty days post SCI, transplantation of hNSC and hFbs was performed. Four injections, 250 nl each, in a concentration containing 75,000 cells/μl of hNSC or 50,000 cells/μl of hFbs in 50% Hank's balanced salt solution and 50% ex-vivo medium were performed bilaterally from the midline, rostral and caudal to the impact site. The control group received injection of buffer solution only.

4.6.2. Results

4.6.2.1. Behavioral assessment. BMS was used to assess locomotor recovery 2 days after the SCI, followed weekly for 4 weeks, and then weekly after the transplantation till sacrifice. The animals were also tested for motor function using BMS scale before inclusion into the study and the animals with motor deficits were excluded. The mice group with hNSC transplantation showed better locomotor recovery as compared to hFbs group and vehicle group. The BMS score at 16 weeks was 6.4 ± 0.4 for hNSC group, 5.6 ± 0.6 for hFbs group, and 4.8 ± 0.5 for vehicle group. Coordination between the forelimb and hindlimb was also compared between the groups. hNSC transplanted group had 64% of mice with improved coordination. 44% of hFbs group and 20% of vehicle group showed improved coordination. Prior to sacrifice, at 16 weeks post SCI, catwalk gait analysis was performed to analyze the swing speed. 1.21 m/s ± 0.06 swing speed was shown by hNSC group as compared to 1.05 m/s ± 0.06 by vehicle group, but hFbs group showed swing speed of 1.13 m/s ± 0.04 and was significantly different from other groups. Allodynia in the hindlimb was tested at15 weeks after the transplantation. Von Frey Hair testing was performed to measure the threshold for withdrawal response with higher force filaments. Recent studies have shown that the astrocytes derived from transplanted NSC have direct correlation with allodynia. The group with hNSC transplant showed a threshold of 6.4 g ± 1.4 as compared to hFbs with 6.0 g ± 0.5 and vehicle group with 6.0 g ± 1.0. This shows no significant difference between the groups, and hence, the group with hNSC transplantation did not have altered threshold response to mechanical allodynia.

4.6.2.2. Histological analysis. The survival and migration of the transplanted cells into the host spinal cord was tested at 16 weeks post transplantation. Optical fractionators probe was utilized to quantify the surviving cells. The group with hNSC transplant showed 215,711 ± 48,978 hNSC on stereological estimate, which is a three times increase from the transplant number of 75,000 cells. The group with hFbs transplant showed 11,701 ± 3070 hFbs, a 4 times decrease in cell count from transplantation number of 50,000 cells. T6-T12 segment of spinal cord (8 mm rostral and 5 mm

Please cite this article in press as: A. Deep, et al., Mouse models of spinal cord injury and stem cell transplantation, Translational Research in Anatomy (2015), http://dx.doi.org/10.1016/j.tria.2015.10.001

caudal from the epicenter of injury) was used to check if hNSC and hFbs migrated into the spinal cord. HNSC migrated up to 8 mm rostral and 5 mm caudal to the injury epicenter as compared to hFbs, which migrated only 2 mm rostral and 2 mm caudally. On quantification of surviving cells at the distal rostral segment, there were 384 hNSC at 8 mm and 697 at 7 mm. At the distal caudal segment there were 1019 hNSC at 4 mm and 244 hNSC at 5 mm. SC121 and Ki67 double labeling of the human cells was performed to see the active cell proliferation capability. Sc121 and Nestin double labeling was also used to see if the cells can retain immaturity at 16 weeks post transplantation. There was a limited proliferation of hNSC, as 2.9% ± 1.06 $SC121^+$ human cells were double-labeled for Ki67 but 31.1% ± 3.23 of cells were double-labeled with SC121 and Nestin, which confirmed their immaturity. Engrafted human cell were also analyzed for Olig2 (immature oligodendrocytes), APC-CC1 (mature oligodendrocytes), βIII-Tubulin (neurons), and GFAP (astrocytes) markers. 34.4% ± 6.38 cells expressed Olig2 and 13.8% ± 1.0 human cells expressed AAP-CCI marker. βIII-Tubulin and GFAP were expressed by 38.1% ± 0.85 and 8.0% ± 1.0 of the $SC121^+$ cells, respectively. Approximately 40.78% of the engrafted cells differentiated into oligodendrocytes (mature and immature lineage). Oligodendrocytes differentiation was primarily in white matter and βIII-Tubulin for neurons was mainly in gray matter. The integration of hNSC with the host was confirmed by confocal and double immunofluorescence for SC121 and contactin-associated protein (CASPR) which shows co-localization of host myelinated axons with CASPR in paranodal protein in white matter, confirming the host and hNSC integration.

5. Conclusion

Mice represent an attractive model for SCI as they are cost effective and can be easily genetically modified. Different mechanisms have been developed to induce SCI, but yet no mechanism was deemed superior. These models have also been used for stem cells therapy trials. Despite differences from human response, animal models, and especially mouse, provides an insight into effectiveness and possible complications of cellular isolation, expansion and transplantation.

Conflict of interest statement

The authors declare that they do not have any conflict of interest.

References

[1] M. Abematsu, K. Tsujimura, M. Yamano, M. Saito, K. Kohno, J. Kohyama, M. Namihira, S. Komiya, K. Nakashima, Neurons derived from transplanted neural stem cells restore disrupted neuronal circuitry in a mouse model of spinal cord injury, J. Clin. Investig. 120 (9) (2010) 3255–3266.
[2] A. Allen, Surgery of experimental lesion of spinal cord equivalent to crush injury of fracture dislocation of spinal column: a preliminary report, J. Am. Med. Assoc. LVII (11) (1911) 878–880.
[3] H. Awad, D.P. Ankeny, Z. Guan, P. Wei, D.M. McTigue, P.G. Popovich, A mouse model of ischemic spinal cord injury with delayed paralysis caused by aortic cross-clamping, Anesthesiology 113 (4) (2010) 880–891.
[4] J.B. Ayer, Cerebrospinal fluid in experimental compression of the spinal cord, Arch. Neurol. Psychiatry 2 (2) (1919) 158–164.
[5] A.R. Blight, Morphometric analysis of a model of spinal cord injury in guinea pigs, with behavioral evidence of delayed secondary pathology, J. Neurol. Sci. 103 (2) (1991) 156–171.
[6] J.E. Coe, T.H. Calvin Jr., F.H. Rudenberg, C.H. Yew, Concussion-like state following cervical cord injury in the monkey, J. Trauma 7 (4) (1967) 512–522.
[7] W.M. Craig, Pathology of experimental compression of the spinal cord, Proc. Staff Meet. Mayo Clin. 7 (1932) 680–682.
[8] U. DeGirolami, J.A. Zivin, Neuropathology of experimental spinal cord ischemia in the rabbit, J. Neuropathol. Exp. Neurol. 41 (2) (1982) 129–149.
[9] T.B. Ducker, H.F. Hamit, Experimental treatments of acute spinal cord injury, J. Neurosurg. 30 (6) (1969) 693–697.
[10] A. Ferraro, Experimental medullary concussion of the spinal cord in rabbits: histologic study of the early stages, Arch. Neurol. Psychiatry 18 (3) (1927) 357–373.
[11] M. Gaviria, H. Haton, F. Sandillon, A. Privat, A mouse model of acute ischemic spinal cord injury, J. Neurotrauma 19 (2) (2002) 205–221.
[12] S. Gelfan, I.M. Tarlov, Physiology of spinal cord, nerve root and peripheral nerve compression, Am. J. Physiol. 185 (1) (1956) 217–229.
[13] J.E. Harvey, H.H. Srebnik, Locomotor activity and axon regeneration following spinal cord compression in rats treated with L-thyroxine, J. Neuropathol. Exp. Neurol. 26 (4) (1967) 661–668.
[14] Y.F. Hu, K. Gourab, C. Wells, O. Clewes, B.D. Schmit, M. Sieber-Blum, Epidermal neural crest stem cell (EPI-NCSC)–mediated recovery of sensory function in a mouse model of spinal cord injury, Stem Cell Rev. 6 (2) (2010) 186–198.
[15] D.L. Kelly Jr., K.R. Lassiter, J.A. Calogero, E. Alexander Jr., Effects of local hypothermia and tissue oxygen studies in experimental paraplegia, J. Neurosurg. 33 (5) (1970) 554–563.
[16] H. Kimura, M. Yoshikawa, R. Matsuda, H. Toriumi, F. Nishimura, H. Hirabayashi, H. Nakase, S. Kawaguchi, S. Ishizaka, T. Sakaki, Transplantation of embryonic stem cell-derived neural stem cells for spinal cord injury in adult mice, Neurol. Res. 27 (8) (2005) 812–819.
[17] P.L. Kuhn, J.R. Wrathall, A mouse model of graded contusive spinal cord injury, J. Neurotrauma 15 (2) (1998) 125–140.
[18] L. Lang-Lazdunski, K. Matsushita, L. Hirt, C. Waeber, J.P. Vonsattel, M.A. Moskowitz, W.D. Dietrich, Spinal cord ischemia. Development of a model in the mouse, Stroke 31 (1) (2000) 208–213.
[19] V.J. Mc, Experimental cord crushes: with especial reference to the mechanical factors involved and subsequent changes in the areas of the cord affected, Arch. Surg. 7 (3) (1923) 573–600.
[20] M.M. Mortazavi, O.A. Harmon, N. Adeeb, A. Deep, R.S. Tubbs, Treatment of spinal cord injury: a review of engineering using neural and mesenchymal stem cells, Clin. Anat. 28 (1) (2015 Jan) 37–44.
[21] M.M. Mortazavi, K. Verma, O.A. Harmon, C.J. Griessenauer, N. Adeeb, N. Theodore, R.S. Tubbs, The microanatomy of spinal cord injury: a review, Clin. Anat. 28 (1) (2015 Jan) 27–36.
[22] Y. Okada, A. Matsumoto, T. Shimazaki, R. Enoki, A. Koizumi, S. Ishii, Y. Itoyama, G. Sobue, H. Okano, Spatiotemporal recapitulation of central nervous system development by murine embryonic stem cell-derived neural stem/progenitor cells, Stem Cells 26 (12) (2008) 3086–3098.
[23] Y. Okada, T. Shimazaki, G. Sobue, H. Okano, Retinoic-acid-concentration-dependent acquisition of neural cell identity during in vitro differentiation of mouse embryonic stem cells, Dev. Biol. 275 (1) (2004) 124–142.
[24] J.R. Plemel, G. Duncan, K.W. Chen, C. Shannon, S. Park, J.S. Sparling, W. Tetzlaff, A graded forceps crush spinal cord injury model in mice, J. Neurotrauma 25 (4) (2008) 350–370.
[25] D.L. Salazar, N. Uchida, F.P. Hamers, B.J. Cummings, A.J. Anderson, Human neural stem cells differentiate and promote locomotor recovery in an early chronic spinal cord injury NOD-scid mouse model, PLoS One 5 (8) (2010) e12272.
[26] H. Schmaus, Beitrage zur pathologischen Anatomie der Ruckenmarkserschut terung, Virchows Arch. 122 (1890) 470–495.
[27] A. Seitz, E. Aglow, E. Heber-Katz, Recovery from spinal cord injury: a new transection model in the C57Bl/6 mouse, J. Neurosci. Res. 67 (3) (2002) 337–345.
[28] T. Seki, K. Hida, M. Tada, I. Koyanagi, Y. Iwasaki, Graded contusion model of the mouse spinal cord using a pneumatic impact device, Neurosurgery 50 (5) (2002) 1075–1081 discussion 1081–1072.
[29] G.N. Sholomenko, J.D. Steeves, Effects of selective spinal cord lesions on hindlimb locomotion in birds, Exp. Neurol. 95 (2) (1987) 403–418.
[30] K. Takahashi, K. Tanabe, M. Ohnuki, M. Narita, T. Ichisaka, K. Tomoda, S. Yamanaka, Induction of pluripotent stem cells from adult human fibroblasts by defined factors, Cell 131 (5) (2007) 861–872.
[31] I.M. Tarlov, H. Klinger, S. Vitale, Spinal cord compression studies. I. Experimental techniques to produce acute and gradual compression, AMA Arch. Neurol. Psychiatry 70 (6) (1953) 813–819.
[32] J.E. Thompson, Pathological changes, occurring in the spinal cord, following fracture dislocation of the vertebrae, Ann. Surg. 78 (2) (1923) 260–293.
[33] J.R. Wrathall, R.K. Pettegrew, F. Harvey, Spinal cord contusion in the rat: production of graded, reproducible, injury groups, Exp. Neurol. 88 (1) (1985) 108–122.
[34] J.D. Yeo, A review of experimental research in spinal cord injury, Paraplegia 14 (1) (1976) 1–11.
[35] J.D. Yeo, W. Payne, B. Hinwood, A.D. Kidman, The experimental contusion injury of the spinal cord in sheep, Paraplegia 12 (4) (1975) 279–298.
[36] J.D. Yeo, W.H. Payne, Sequential pathological changes seen in controlled trauma to the spinal cord of the sheep, Ann. Meeting Royal College of Pathologists of Aust., Auckland, N.Z, J. Pathol. 7 (1975) 66.

Please cite this article in press as: A. Deep, et al., Mouse models of spinal cord injury and stem cell transplantation, Translational Research in Anatomy (2015), http://dx.doi.org/10.1016/j.tria.2015.10.001